Reconstitution of *UCP1* using CRISPR/Cas9 in the white adipose tissue of pigs decreases fat deposition and improves thermogenic capacity

Qiantao Zheng[a,b,1], Jun Lin[c,d,1], Jiaojiao Huang[a,b,1], Hongyong Zhang[a,b], Rui Zhang[a,b], Xueying Zhang[e], Chunwei Cao[a,b], Catherine Hambly[f], Guosong Qin[a,b], Jing Yao[a,b], Ruigao Song[a,b], Qitao Jia[a,b], Xiao Wang[a,b], Yongshun Li[a], Nan Zhang[a], Zhengyu Piao[g], Rongcai Ye[c,d], John R. Speakman[e,f], Hongmei Wang[a,b], Qi Zhou[a,b], Yanfang Wang[h,2], Wanzhu Jin[b,c,2], and Jianguo Zhao[a,b,2]

[a]State Key Laboratory of Stem Cell and Reproductive Biology, Chinese Academy of Sciences, Chaoyang District, Beijing, China 100101; [b]Savaid Medical School, University of Chinese Academy of Sciences, Beijing, China 100049; [c]Key Laboratory of Animal Ecology and Conservation Biology, Chinese Academy of Sciences, Chaoyang District, Beijing, China 100101; [d]College of Life Science, University of Chinese Academy of Sciences, Beijing, China 100049; [e]Institute of Genetics and Developmental Biology, Chinese Academy of Sciences, Beijing, China 100101; [f]Energetics Research Group, Zoology Department, University of Aberdeen, Aberdeen AB24 2TZ, United Kingdom; [g]Department of Animal Science, Yanbian University, Yanji, Jilin, China 133002; and [h]Institute of Animal Science, Chinese Academy of Agricultural Sciences, Beijing, China 100193

Edited by R. Michael Roberts, University of Missouri-Columbia, Columbia, MO, and approved September 14, 2017 (received for review May 12, 2017)

Uncoupling protein 1 (UCP1) is localized on the inner mitochondrial membrane and generates heat by uncoupling ATP synthesis from proton transit across the inner membrane. UCP1 is a key element of nonshivering thermogenesis and is most likely important in the regulation of body adiposity. Pigs (Artiodactyl family *Suidae*) lack a functional UCP1 gene, resulting in poor thermoregulation and susceptibility to cold, which is an economic and pig welfare issue owing to neonatal mortality. Pigs also have a tendency toward fat accumulation, which may be linked to their lack of UCP1, and thus influences the efficiency of pig production. Here, we report application of a CRISPR/Cas9-mediated, homologous recombination (HR)-independent approach to efficiently insert mouse adiponectin-UCP1 into the porcine endogenous *UCP1* locus. The resultant UCP1 knock-in (KI) pigs showed an improved ability to maintain body temperature during acute cold exposure, but they did not have alterations in physical activity levels or total daily energy expenditure (DEE). Furthermore, ectopic UCP1 expression in white adipose tissue (WAT) dramatically decreased fat deposition by 4.89% ($P < 0.01$), consequently increasing carcass lean percentage (CLP; $P < 0.05$). Mechanism studies indicated that the loss of fat upon UCP1 activation in WAT was linked to elevated lipolysis. UCP1 KI pigs are a potentially valuable resource for agricultural production through their combination of cold adaptation, which improves pig welfare and reduces economic losses, with reduced fat deposition and increased lean meat production.

UCP1 | thermoregulation | fat deposition | pig | CRISPR/Cas9

Uncoupling protein 1 (UCP1) serves as a proton leak across the inner mitochondrial membrane. This process contributes to energy dissipation as heat; thus, UCP1 plays a key role in brown adipose tissue (BAT)-mediated adaptive nonshivering thermogenesis (NST) (1). The roles of BAT and UCP1 in energy expenditure and metabolic diseases, such as obesity and type 2 diabetes, have been extensively investigated (1, 2). A role for UCP1 in resistance against obesity was postulated from the results of studies in genetically modified mice (1, 3, 4), and UCP1 is also implicated in the pathogenesis of obesity and metabolic disorders in humans (5–7).

UCP1 is present in most eutherian mammals, but it has been lost in both birds and reptiles and was independently lost in several mammalian lineages, including pigs (8). The loss of *UCP1* in the pig lineage has been well documented (9–12). A genetic event eliminating exons 3–5 occurred ∼20 million y ago when the ancestral Suidae were living in tropical and subtropical environments, where they could survive without UCP1-mediated NST (10). For pig production, the litter must be provided with a warm microenvironment, and the wild sow is the only ungulate that builds a thermoprotective nest for giving birth (13, 14). The disruption of the *UCP1* gene in pigs consequently resulted in a lack of functional BAT (15). This evolutionary history has important practical implications for the pig industry. First, modern pigs struggle with poor thermoregulation, leading to significant neonatal mortality of piglets caused by cold stress at birth. This is a major welfare and energy expenditure issue for the swine industry in cold regions worldwide. Supplemental heat, such as heat lamps, had to be provided to warm the preweaning piglets, which totals to ∼35% of the energy cost in swine farrow-to-finish operations, bringing about an annual expenditure of $99.3 million with heat lamps for 94 million hogs marketed in the United States (16). Moreover, the involvement of UCP1 in the pathogenesis of obesity may explain the high levels of fat deposition in pigs. Fat deposition is an economically important trait, influencing pork production, meat quality, dietetic value, and growth efficiency (17). Pig breeding programs have long focused on

Significance

Uncoupling protein 1 (UCP1) is responsible for brown adipose tissue-mediated thermogenesis and plays a critical role in protecting against cold and regulating energy homeostasis. Modern pigs lack functional UCP1, which makes them susceptible to cold and prone to fat deposition and results in neonatal mortality and decreased production efficiency. In the current study, a CRISPR/Cas9-mediated homologous recombination-independent approach was established, and mouse adiponectin-UCP1 was efficiently inserted into the porcine endogenous *UCP1* locus. The resultant UCP1 KI pigs showed an improved ability to maintain body temperature, decreased fat deposition, and increased carcass lean percentage. UCP1 KI pigs are a potentially valuable resource for the pig industry that can improve pig welfare and reduce economic losses.

Author contributions: Q. Zhou, Y.W., W.J., and J.Z. designed research; Q. Zheng, J.L., J.H., H.Z., R.Z., X.Z., C.H., G.Q., J.Y., R.S., Q.J., X.W., Y.L., N.Z., Z.P., R.Y., J.R.S., and H.W. performed research; Q. Zheng, J.L., X.Z., C.C., J.R.S., H.W., Q. Zhou, Y.W., and J.Z. analyzed data; and Q. Zheng, J.R.S., Y.W., and J.Z. wrote the paper.

Conflict of interest statement: J.Z., Q. Zheng, J.H., G.Q. and W.J. have a pending patent application "Production of transgenic pigs tolerant to cold stimulation with lean phenotype."

This article is a PNAS Direct Submission.

[1]Q. Zheng, J.L., and J.H. contributed equally to this work.

[2]To whom correspondence may be addressed. Email: wangyanfang@caas.cn, jinw@ioz.ac.cn, or zhaojg@ioz.ac.cn.

This article contains supporting information online at www.pnas.org/lookup/suppl/doi:10.1073/pnas.1707853114/-/DCSupplemental.

genetic selection toward less fat deposition and increased leanness, which holds great promise for high-efficiency pig production (18).

In theory, restoring functional UCP1 in the domestic pig could improve thermoregulation and decrease fat deposition to benefit both pig welfare and production. However, it is extremely difficult to perform site-specific genome engineering in mammalian species that lack characterized embryonic stem cells for a classical homologous recombination (HR)-targeting strategy. With the recent development of the CRISPR/Cas9 system, precision genome editing involving site-specific, HR-dependent knock-in (KI) has been reported in mice (19) and would become feasible in pigs (20).

In this study, we generated white adipose tissue (WAT)-specific UCP1 KI pigs using CRISPR/Cas9-mediated site-specific integration, which is independent of HR. We found that these pigs exhibited significantly improved thermoregulation. Most strikingly, the ectopic expression of UCP1 decreased fat deposition without altering physical activity or daily energy demands. This study highlights the potential for biotechnology use in pig breeding to improve cold resistance and lean pork production.

Results

Generation of Adiponectin-UCP1 KI Pigs and Germline Transmission of the Transgene. The absence of functional UCP1 in Bama pigs, a southern Chinese native and cold-sensitive breed, was confirmed by protein sequence alignment, which showed the absence of exons 3–5 (Fig. S1*A*), and by semiquantitative PCR, which could not detect UCP1 transcription in various adipose depots (Fig. S1*B*).

A CRISPR/Cas9-mediated, HR-independent integration strategy was used and developed to insert UCP1 into the porcine endogenous *UCP1* locus. A UCP1 expression and targeting vector containing bait sequence (the same sequence as the Cas9 target site in the genomic locus) and mouse UCP1 cDNA driven by the adipose tissue-specific adiponectin promoter was constructed according to a previous report (21) (Fig. 1*A*). Briefly, the adiponectin-UCP1 3′ UTR fragment was subcloned into a positive lethal-based (PLB) backbone plasmid and the bait sequence was then inserted (Fig. 1*A*, labeled in blue); that is, the single-guide RNA (sgRNA) target site (capital letters in rectangular frame) and the protospacer adjacent motif sequence (flanking 3′ end of the DNA target site required for Cas9 recognizing, lowercase letters in rectangular frame) were inserted in front of the adiponectin promoter sequence (Fig. 1*A*). A Cas9-guide RNA (gRNA) plasmid targeting the endogenous *UCP1* was also constructed as previously demonstrated (22).

The schematic for the production of KI pigs is shown in Fig. 1*B*. The Cas9-gRNA plasmid and targeting vector were cotransfected into pig embryonic fibroblast cells (PEFs), and cells were then distributed into a 96-well plate by a limiting dilution method to distribute one cell in each well. Transfected cells were propagated and genotyped using primers designed to identify forward integration (P1/P2 for 5′ junction, P3/P4 for 3′ junction; Fig. 1*A*). Three of 26 cell colonies were identified as positive for forward integration (11.54%), and cell colony no. 17 was used as donor cells for somatic cell nuclear transfer (SCNT) (Fig. S2).

A total of 2,553 cloned embryos were transferred into the oviducts of 13 recipient surrogates. Three pregnancies were established and went to term. Twelve male piglets were born by natural delivery from three litters (Table S1), and the representative pigs are shown in Fig. 1*C*. UCP1 KI was identified by PCR genotyping (Fig. 1*D*) and was further confirmed by measuring *UCP1* mRNA (Fig. 1*E*) and protein (Fig. 1*F*) expression in inguinal s.c. fat depots in the KI pigs. No expression of foreign *UCP1* was observed in other tissues, such as the heart, liver, spleen, lung, kidney, muscle, or testis (Fig. S1*D*).

One UCP1 KI founder was mated to two wild-type (WT) Bama female pigs and gave birth to 15 first-generation (F_1) offspring. PCR analysis revealed that eight of the 15 F_1 pigs carried a single copy of UCP1 transgene, showing Mendelian segregation of transgenes among the F_1 progeny (Fig. S1*C*). These results confirmed the feasibility of germline transmission of CRISPR/Cas9-based genetic engineering in pigs and showed that UCP1 KI might not alter fertility.

UCP1 KI Pigs Exhibited Improved Thermoregulation. ^{18}F-Fluorodeoxyglucose (^{18}F-FDG) positron emission tomography (PET) imaging is routinely used to investigate UCP1-dependent BAT activity (23, 24). To test the ability of UCP1 KI piglets to cope with a cold environment, 1-mo-old WT and KI piglets were housed at either room temperature (RT) or 4 °C for 4 h before being injected with ^{18}F-FDG through the ear vein. Positive signals from PET were analyzed to compare ^{18}F-FDG uptake between WT and KI pigs. There were no positive PET signals observed in either WT or KI pigs at RT, whereas the uptake of ^{18}F-FDG was dramatically increased in both the abdomen and inguinal s.c. fat areas of the KI pigs after cold exposure (Fig. 2*A*).

Next, a time-course cold challenge experiment was conducted with 1-mo-old WT and KI piglets (n = 6 per group), and the rectal temperatures were monitored. As shown in Fig. 2*B*, the body temperatures of UCP1 KI piglets dropped from 39.4 ± 0.16 °C to 38.4 ± 0.24 °C after 1 h of cold exposure and then remained above 38 °C throughout the 4-h test period. However, the WT piglets displayed a continued decrease in body temperature for the first 2 h of cold exposure. The WT piglets' temperatures recovered slightly in hours 3 and 4 but remained significantly lower than those from KI piglets ($P < 0.01$ for comparison at 3 h and $P < 0.05$ at 4 h; Fig. 2*B*). In addition, ventral infrared thermal images of both WT and KI pigs were collected at 0, 2, and 4 h during the cold challenge (n = 4 per group; Fig. S3*D*). The average surface temperatures of three specific areas (labeled 1, 2, and 3) were calculated, and the quantification is shown in Fig. S3*E*. Significantly improved body temperature maintenance was clearly indicated by the higher body temperatures in all three areas of KI pigs during cold exposure (Fig. S3*E*). The cold challenge experiment was repeated when these pigs were 6 mo old (n = 6 per group). Additionally, higher rectal temperatures were observed in KI pigs compared with WT pigs during cold exposure (Fig. S3*A*). Infrared thermal images of ventral (Fig. 2*C*) and dorsal (Fig. S3*B*) sides were collected (n = 4 per group), and in agreement with the observations in 1-mo-old piglets, KI pigs exhibited higher surface body temperatures (Fig. 2*D* and Fig. S3*C*).

Ectopic Expression of UCP1 Enhances Mitochondrial Function in Adipose Tissue. UCP1 expression in BAT is tightly correlated with mitochondrial number and/or function. To investigate the effects of ectopic UCP1 expression in porcine adipose tissues on mitochondrial functions, preadipocytes from WT and KI pigs were successfully isolated and differentiated into mature adipocytes in vitro (Fig. S4*A*). Oil-red-O staining indicated that there were no significant differences in differentiation efficiency between the two groups (Fig. S4*A*), which was further confirmed by equivalent mRNA and protein expression levels of the adipogenic markers FABP4 (*AP2*) and *PPARγ* (Fig. S4 *B* and *C*). Western blot results confirmed that UCP1 was detectable only in the adipocytes from KI pigs (Fig. S4*C*). To assess mitochondrial activity, we analyzed the cellular bioenergetics profile using a Seahorse XF24 analyzer, and data revealed that despite a similar basal oxygen consumption rate (OCR) in both WT and KI cells (P = 0.99; Fig. 2*E*, *Middle*), the addition of the exogenous uncoupler carbonyl cyanide-4-(trifluoromethoxy) phenylhydrazone (FCCP) increased OCR to a higher level in KI cells than in WT cells (P = 0.01; Fig. 2*E*, *Left*). As such, UCP1 KI adipocytes displayed significantly higher maximal respiration (fold change = 1.62, P = 0.01; Fig. 2*E*, *Right*), suggesting that ectopic

UCP1 expression increased the spare respiratory capacity of the mitochondria.

Ectopic Expression of UCP1 Did Not Alter Physical Activity or Daily Energy Expenditure. Elevated UCP1 expression may lead to changes in the overall energy budget as a result of greater heat production. If heat production was excessive, it might, for example, lead to reduced physical activity to avoid hyperthermia, and thus alter total daily energy expenditure (DEE). Physical activity levels were monitored using activity loggers (GT3x), which record movements in three dimensions on a minute-by-minute time frame. There was a strong effect of time of day on physical activity levels ($F_{23,161} = 7.96$, $P < 0.001$) and a significant random effect for individual nested within genotype ($F_{6,161} = 17.39$, $P < 0.001$). However, UCP1 KI and WT pigs did not differ significantly in their overall physical activity levels ($n = 4$ per group; genotype effect: $F_{1,161} = 1.74$, $P = 0.19$; Fig. 2*F*). The time-by-genotype interaction was also not significant ($F_{23,144} = 0.3$, $P = 0.99$), suggesting that routine heat production by the ectopically expressed UCP1 was not great enough to reduce activity as a protective measure against increased risk of hyperthermia.

We measured DEE in unconstrained UCP1 KI and WT pigs using the doubly labeled water (DLW) method ($n = 6$ per group) (25). There was no difference between the WT and UCP1 KI animals once the body mass effect had been taken into account using analysis of covariance (26) ($F_{1,9} = 0.01$, $P = 0.95$; Fig. 2*G*). The body weight-by-genotype interaction was not significant ($F_{1,8} = 0.12$, $P = 0.74$). Similar results were obtained when the lean tissue mass was used as the predictor variable (lean tissue effect: $F_{1,9} = 15.09$, $P = 0.006$; genotype: $F_{1,9} = 0.13$, $P = 0.73$). Fat mass did not explain any of the variation in DEE once the effect of lean mass was accounted for ($F_{1,8} = 0.1$, $P = 0.76$).

Decreased Fat Deposition and Increased Adipose Lipolysis in UCP1 KI Pigs. Fat deposition is an important economic trait in pigs, and reducing fat deposition has been a major objective in pig breeding programs. Owing to the critical role of UCP1 in energy hemostasis and fat deposition, we were particularly interested in whether UCP1 expression would affect fat deposition in KI pigs. There was no significant difference in body weight between the different genotypes at birth (0.52 ± 0.14 kg for WT vs. 0.49 ± 0.06 kg for KI, $P = 0.63$) or at 6 mo old (27.50 ± 3.23 kg for WT vs. 25.67 ± 0.86 kg for KI, $P = 0.25$) ($n = 6$ for WT and $n = 5$ for KI; Fig. 3*A*), which indicated that the growth rate of KI pigs was not affected significantly. There was also no significant change in the feed conversion ratio (FCR) during ad libitum feeding (WT pigs: FCR = 3.04 ± 0.13, $n = 6$; KI pigs: FCR = 3.12 ± 0.06, $n = 5$; $P = 0.59$; Fig. 3*B*), consistent with the absence of an effect on the DEE. These pigs ($n = 6$ for WT and $n = 5$ for KI) were slaughtered at 6 mo of age, and the left half of each carcass was dissected for further analysis. The detailed slaughter indexes are shown in Table S2. Strikingly, the ratio of lean meat to carcass weight [CW; carcass lean percentage (CLP)] was increased by 3.38% in KI pigs (53.12 ± 1.01% for KI vs. 49.74 ± 2.43% for WT; $P = 0.03$). The ratios of fat content to the CW [carcass fat percentage (CFP)] were 15.28 ± 3.11% and 20.17 ± 1.80% ($P = 0.01$) for KI and WT pigs, respectively, which corresponded to a 24% reduction for UCP1 KI pigs (Fig. 3*C* and Table S2). In

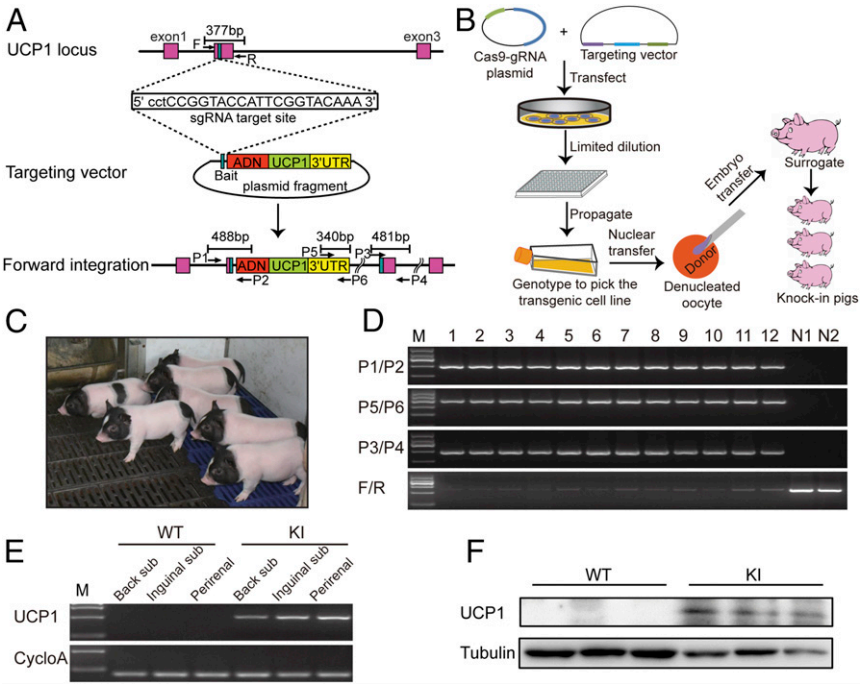

Fig. 1. CRISPR/Cas9-mediated, HR-independent integration efficiently produces adiponectin (ADN)-UCP1 KI pigs. (*A*) Schematic representation of the design of the targeting vector. Exons of *UCP1* are shown as purple-red boxes, and the cyan box in exon 2 represents the sgRNA targeting site, which is enlarged to a rectangle box with the protospacer adjacent motif sequence labeled in lowercase and the targeting sequence in capital letters. The cyan box in the targeting vector is the same as the one in exon 2, which is also called the bait sequence. Red and yellow boxes representing the ADN promoter and the 3′ UTR constitute the promoter element, and UCP1 in green is located in the middle. Forward integration occurs if the 5′ site at the DSB of the targeting vector is ligated behind the 3′ site of the DSB in the *UCP1* locus. Four pairs of primers are designed for genotyping. P1/P2 and P3/P4 are designed for genotyping the 5′ and 3′ junctions in the transgenic colonies, respectively. P5/P6 and F/R primers are designed for detecting the donor vector region and undamaged genomic sequence in the cloned pigs, respectively. (*B*) Schematic overview of the production of KI pigs. (*C*) KI pigs at day 15. (*D*) PCR genotyping-confirmed site-specific insertion of donor DNA in the cloned pigs. Lanes 1–12 represent 12 individuals, and lanes N1 and N2 represent two negative control WT pigs. (*E*) Semiquantitative PCR analysis of *UCP1* from WT and KI adipose tissue to assess the expression of the foreign gene. Back sub, back s.c. fat; Inguinal sub, inguinal s.c. fat. (*F*) Western blot analysis confirmed UCP1 expression in the KI pigs ($n = 3$).

agreement with a reduced CFP, significantly thinner back fat [back fat thickness (BFT)] was observed in KI pigs; it was 2.44 mm thinner compared with WT pigs (n = 4 per group, 6.84 ± 0.45 mm for KI vs. 9.28 ± 0.13 mm for WT; P = 0.002), which corresponded to a 26% reduction for UCP1 KI pigs (Fig. 3*D* and Table S2).

To investigate why fat accumulation was reduced in UCP1 KI pigs, fat tissues from different depots, including back, inguinal s.c., and perirenal depots, were collected from WT and KI pigs and subjected to hematoxylin and eosin (H&E) staining and transmission electron microscopy (TEM) analysis. UCP1 activation in the WAT can promote WAT browning (called beige cells) to prevent diet-induced obesity (27, 28). In the current study, no obvious beige cells were observed by H&E staining in various fat deposits from UCP1 KI pigs, and the expression levels of beige-related genes in WAT were not altered (Fig. S5). However, KI adipocytes from these depots were significantly smaller compared with those from WT pigs (Fig. 4*A*), and TEM analysis showed that many small lipid droplets were found in KI adipocytes, whereas WT adipocytes contained fewer larger droplets (Fig. 4*B*). Furthermore, the mitochondrial copy number was not altered in the inguinal s.c. fat (n = 4 per group, 448.4 ± 71.8 for WT vs. 466.8 ± 59.6 for KI; P = 0.85) or perirenal fat (n = 4 per group, 985.5 ± 269.2 for WT vs. 983.6 ± 70.4 for KI; P = 0.99) based on the qPCR analysis of the mitochondrial *COX2* gene relative to *β-globin* (Fig. 4*D*). The presence of small

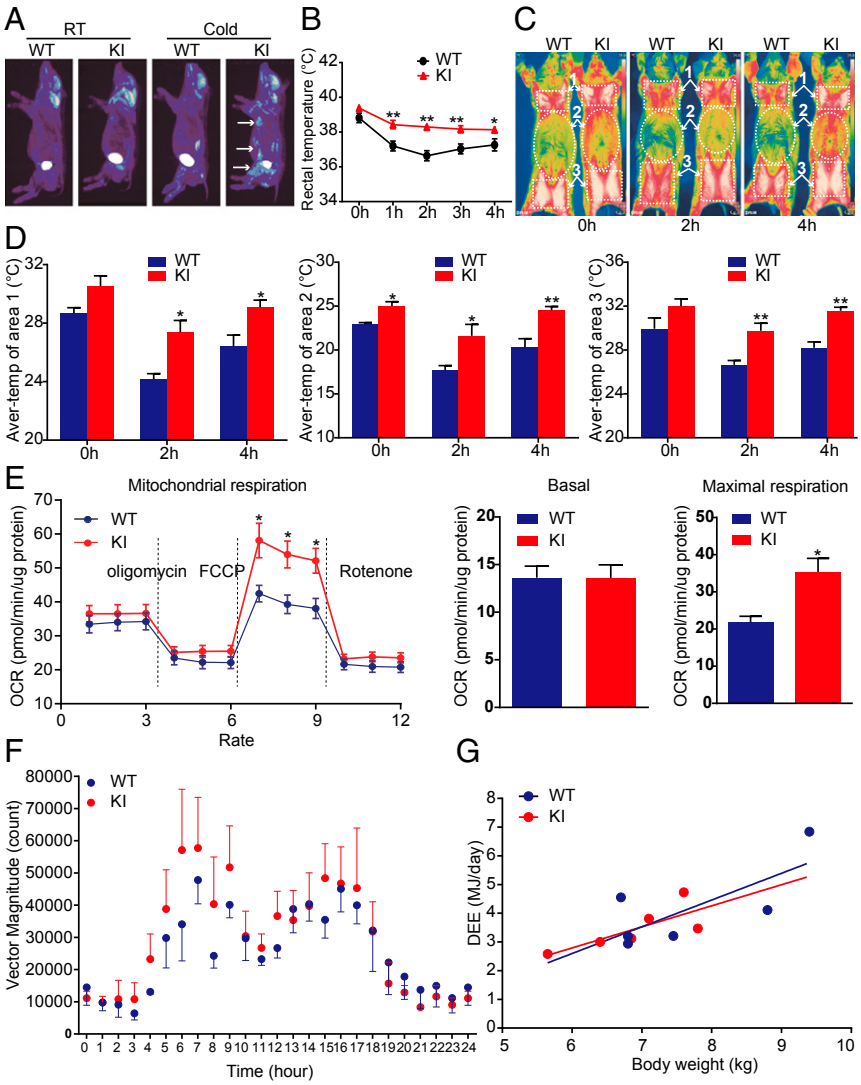

Fig. 2. Ectopic expression of UCP1 improves thermoregulation in pigs. (*A*) PET analysis of 1-mo-old WT and KI piglets at RT or after cold stimulation (Cold). Positive signals were identified in KI pigs after cold exposure, as indicated by white arrows. (*B*) Rectal temperature monitor of 1-mo-old WT (n = 6) and KI (n = 6) piglets during cold stimulation for 4 h revealed that KI pigs were more tolerant to cold challenge. (*C*) Infrared pictures were taken at 0, 2, and 4 h after cold exposure in 6-mo-old pigs. The white-dotted lines depict areas labeled 1, 2, and 3, where temperatures were quantified. Higher temperature could be observed in KI pigs from the thermal picture. (*D*) Temperature quantification of areas 1, 2, and 3 in WT and KI (n = 4 per group) pigs at different time points. Aver-temp, average temperature. (*E*) OCR in differentiated white adipocytes from WT and KI pigs showed similar basal cellular respiration but higher maximal respiration in KI cells. (*F*) Physical activity levels (vector magnitude counts) using the GT3x accelerometer in live pigs as a function of time of day. Red points are UCP1 KI transgenic pigs (n = 4), and blue points are WT controls (n = 4). There was no effect of genotype on physical activity levels. (*G*) DEE (megajoules per day) assessed by the DLW technique for free-roaming pigs relative to body weight. The red points and red line (fitted regression) are UCP1 KI transgenic pigs (n = 6), and the blue points and blue line are WT controls (n = 6). There was a strong effect of body weight but no effect of genotype on DEE. Values are shown as the mean ± SEM; significant differences compared with controls are indicated by $^{**}P < 0.01$ and $^{*}P < 0.05$. Data were analyzed with a two-sample t test. In *F* and *G*, the data were analyzed by general linear models.

lipid droplets indicated that lipolysis may be enhanced in KI adipocytes, and in vitro lipolysis assays showed that under both basal and isoproterenol-stimulated conditions, the release of glycerol from inguinal s.c. fat explants isolated from UCP1 KI pigs ($n = 4$ per group, 0.48 ± 0.08 nmol/mg at basal conditions and 1.2 ± 0.06 nmol/mg after stimulation) was significantly higher, by twofold and 1.5-fold, respectively, compared with WT pigs ($n = 4$ per group; 0.22 ± 0.02 nmol/mg at basal conditions, $P = 0.02$; 0.75 ± 0.05 nmol/mg after stimulation, $P = 0.001$; Fig. 4 *C* and *E*). Moreover, the UCP1 KI pigs showed significantly higher plasma free fatty acid (FFA) levels ($n = 3$ per group, 0.35 ± 0.03 for KI vs. 0.21 ± 0.03 for WT; $P = 0.01$) and lower triglycerides (TGs; $n = 3$ per group, 0.18 ± 0.03 for KI vs. 0.29 ± 0.01 for WT; $P = 0.006$) without any stimulation (Fig. 4*G*). Furthermore, the expression levels of phosphohormone-sensitive lipase (pHSL) and adipose triglyceride lipase (ATGL), two well-recognized lipolysis rate-limiting enzymes, were also significantly increased in UCP1 KI pigs (Fig. 4*F*). Taken together, these data suggested that there was increased lipolysis in the UCP1 KI pigs.

Discussion

Genome editing in pigs is of considerable importance for potential applications in pig production. Recent progress in nuclease-mediated genome editing, such as CRISPR/Cas9 technology, provides a precise and highly efficient method for editing in cells, tissues, and whole organisms (29). Undoubtedly, breeding and trait improvements in livestock will be accelerated by CRISPR-based genome engineering. For example, by deleting *CD163* with CRISPR/Cas9, pigs have been created that are protected against porcine reproductive and respiratory syndrome virus (30). The random integration of a foreign gene into a different genome often results in unstable phenotypes, gene silencing, and unpredictable gene expression patterns, and this process is mutagenic in some cases (31). Therefore, producing animals that carry exogenous genes integrated at specific genomic loci is far superior (32). CRISPR/Cas9 mediated double-strand break (DSB) that facilitates HR-dependent insertions of exogenous DNA sequences into a specific locus in pigs has been successfully reported (33, 34). However, HR is inefficient in many cell types, even when a site-specific DSB is mediated by nucleases (31). To overcome the low efficiency of HR-mediated KI, Li et al. (21) developed a genetic modification method in zebrafish using nonhomologous end joining, which has a much higher efficiency than HR. However, until now, this strategy has not been tested and reported in pigs.

In this study, combined with SCNT, we efficiently inserted an adiponectin-UCP1 fragment at the length of 9 kb into the porcine endogenous *UCP1* locus by a CRISPR/Cas9-mediated, HR-independent approach. During the process of making genetic modifications in the PEFs, three of 26 colonies were genotyped as positive for the successful insertion, which corresponded to a KI efficiency of ~11.5%. All of the 12 offspring were genotyped transgene-positive as anticipated. These data indicated that this approach could efficiently insert a foreign fragment as large as 9 kb at a specific locus. However, junction sequencing analysis revealed some mismatches at both the 5′ and 3′ insertion sites, suggesting that this approach might not be suitable for precision insertion.

Adaptive NST generated in BAT enables small eutherian mammals and the neonates of large animals to maintain a high body temperature (35). Most likely because of their tropical evolutionary history, pigs lost functional UCP1 in a genetic event. In the current study, we confirmed that neither classical BAT nor detectable *UCP1* gene expression was observed in neonatal Bama piglets. Correspondingly, it was previously shown that body temperature regulation in the piglet does not rely on BAT-derived NST, but is primarily dependent on shivering thermogenesis from skeletal muscle (36). Other reports have shown that the newborn piglet usually experiences a sudden and dramatic 15–20 °C decrease in its thermal environment. Without protection against climatic influences, the piglets would experience hypothermia, which is a leading cause of neonatal death (37). Research in 2011 reported that farmers suffered an average 20% mortality per litter of piglets, with one major cause being chilling, although heat lamps had been used to provide localized heating for piglets (38–40). Neonatal piglet survival has decreased over the last 20 y with increasing litter size; thus, it remains a major problem in modern pig production (41) and could lose more than €50,000 per year in a farm with a herd of 250 sows (13). The need to improve pig thermoregulation for better neonatal survival rate prompted us to hypothesize that ectopic UCP1 expression in adipocyte tissues could be an attractive approach to enhance the ability of piglets to resist cold stress. Our data confirmed the hypothesis that ectopic UCP1 expression in the WAT enhanced the thermogenic capacity of piglets, and they were able to maintain their body temperature much better than WT pigs during acute exposure to cold (4 °C). These data are consistent with the observation that UCP1 knockout mice are unable to maintain their body temperature when acutely exposed to cold (42). In the pig industry, a balance must be struck between the thermal needs of the sow and her litter (13). The optimal temperature zone for the sow is 22–25 °C, and evaporative cooling is required to prevent her body temperature from increasing; otherwise, feed intake and milk production are decreased (43, 44). Thus, the current UCP1 KI pig might provide a solution by keeping the piglets in the lower ambient temperature without affecting their survival and without inducing heat stress for the sow.

A potential converse problem of overexpressing UCP1 in WAT is that the animals might produce too much heat. This would lead to increased DEE, a reduced FCR, and a risk of hyperthermia. Animals may then attempt to mitigate this hyperthermia risk by

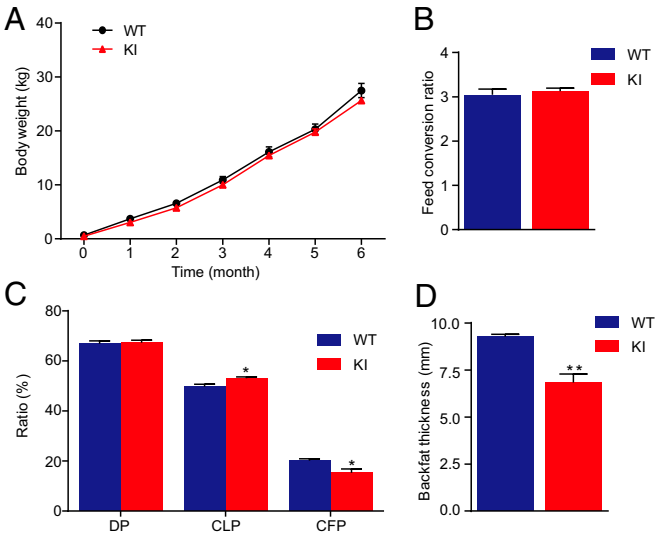

Fig. 3. Ectopic expression of UCP1 decreases fat deposition in pigs. (*A*) Growth curve from birth to 6 mo of age showing no difference in body weight between WT ($n = 6$) and KI ($n = 5$) pigs. A growth spurt occurs at 2 mo because of the start of ad libitum feeding at this time. (*B*) There is no difference between the FCR ratio of WT ($n = 6$) and KI ($n = 5$) pigs during the ad libitum feeding period. (*C*) Proportion of carcass to body weight (DP, dressing percentage), lean meat to left half of the carcass (CLP), and fat to left half of the carcass (CFP) for WT ($n = 6$) and KI ($n = 5$) pigs. The DP showed no difference, but a higher CLP and lower CFP were found in KI pigs. (*D*) BFT, converted to that of 20 kg of body weight, is significantly thinner in KI pigs ($n = 4$) than in WT pigs ($n = 4$). Values are shown as the mean ± SEM; significant differences compared with controls are indicated by $^{**}P < 0.01$ and $^{*}P < 0.05$. Data were analyzed with a two-sample *t* test.

reducing their physical activity levels. Strikingly, we did not observe significant changes in the daily energy demands and FCR of the UCP1 KI pigs relative to WT pigs, and there was no diminution in physical activity levels of the transgenic pigs. These results suggest that the in vivo activity of the inserted UCP1 is relatively low and safe with respect to hyperthermia risk.

Besides thermoregulation, intact function of BAT is an important mechanism in small mammals to protect them from diet-induced obesity and diabetes (45). Mice lacking BAT are susceptible to obesity, whereas mice with increased BAT function or elevated *UCP1* mRNA stability are protected against high-fat diet–induced obesity (1, 28, 46, 47). In humans, increased body mass index is correlated with decreased BAT activity (48, 49). These studies suggested that ectopic UCP1 expression may not only improve thermoregulation but also have beneficial effects on fatness and carcass traits in the transgenic pigs. The fatness traits are important in pig production because they are related to meat quality and feed efficiency. For a long time, the major objective of pig breeding programs was to increase the carcass meat percentage for higher feed efficiency since approximately fourfold as much energy is required to grow 1 kg of fat tissue compared with 1 kg of lean tissue (18). BFT and CFP are the most important fatness traits considered in pig breeding improvement and are negatively correlated to lean percentage (50, 51). Fat-type pig breeds, including European breeds, such as Mangalica and the Iberian pigs (52), and Chinese breeds, such as Erhualian, Meishan, and Bama pigs (53), produce high-quality meat with desirable palatability attributes, but they have poor

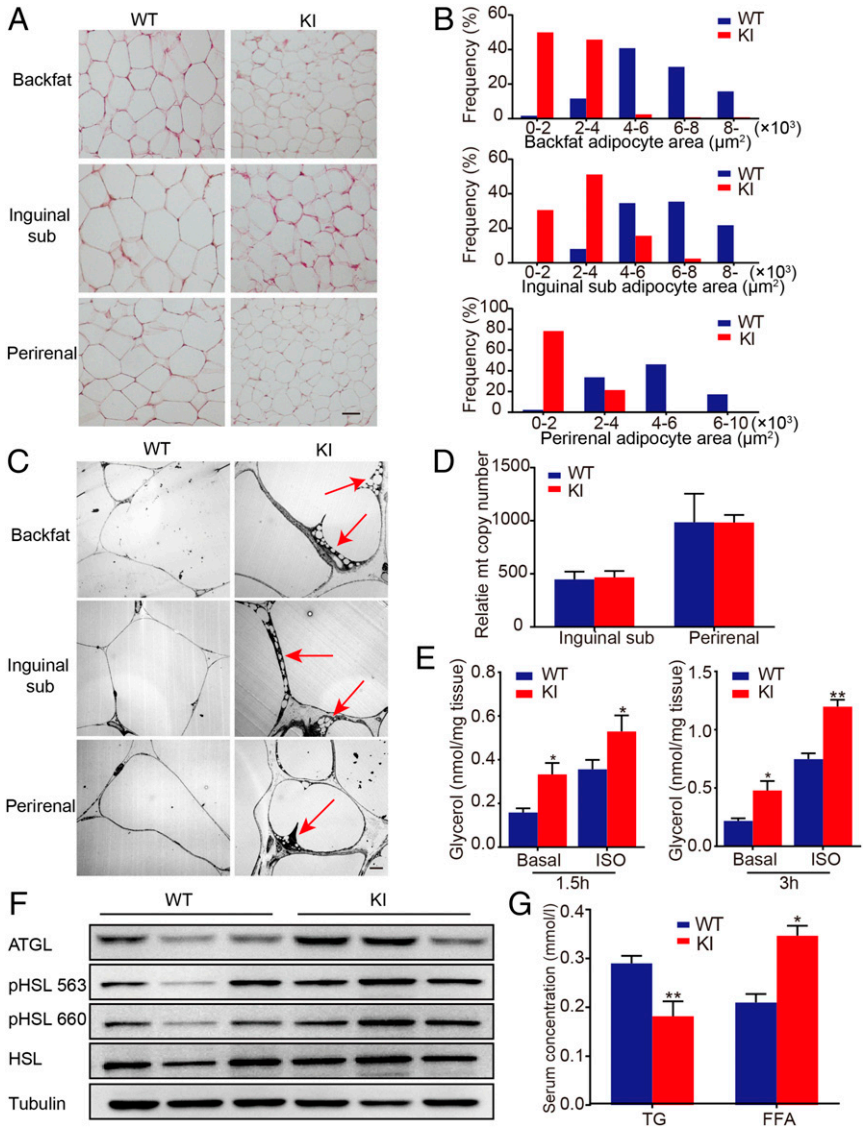

Fig. 4. Ectopic expression of UCP1 promotes lipolysis. (*A*) H&E staining of adipocytes from backfat (*Upper*), inguinal subfat (sub; *Middle*), and perirenal fat (*Lower*) depicted smaller fat cells in KI pigs. (Scale bar: 50 μm.) (*B*) Distribution of fat cell size from the three fat depots in WT and KI pigs. At least 200 fat cells were counted in each genotype. (*C*) TEM analysis of adipocytes from backfat (*Upper*), inguinal sub (*Middle*), and perirenal fat (*Lower*). Small lipid droplets indicated by red arrows were identified in KI adipocytes. (Scale bar: 5 μm.) (*D*) Relative mitochondria copy number analysis of inguinal sub and perirenal fat showed no difference between the two genotypes ($n = 4$ per group). (*E*) Measurement of glycerol release in inguinal sub at 1.5 h and 3 h showed higher content in KI pigs either at the basal level or after isoproterenol (ISO) stimulation ($n = 4$ per group). (*F*) Western blot analysis showed higher expression levels of ATGL, pHSL, and HSL protein in KI inguinal sub compared with WT ($n = 3$ per group). (*G*) Serum concentration of TGs was significantly decreased, whereas increased FFAs were seen in KI pigs ($n = 3$ per group). Values are shown as the mean ± SEM; significant differences compared with controls are indicated by $^{**}P < 0.01$ and $^{*}P < 0.05$. Data were analyzed with a two-sample *t* test.

production characteristics, such as slow growth rate, lower feed efficiency, and less ideal carcass composition because of extreme levels of fat (54). The improvement of fatness traits of these breeds is a necessary step to improve the total efficiency of pork production. Although for commercial pig breeds that are designated "lean type," such as Large White, Landrace, and Duroc pigs, the fatness traits have been improved greatly by long-term selection with a conventional breeding approach, and the addition of ractopamine hydrochloride improves their growth performance and carcass characteristics, suggesting that even lean-type commercial pig breeds have room for further improvement in pig fatness traits (55).

Our data confirmed that UCP1 expression dramatically decreased the CFP (4.89% less) and BFT (2.44 mm less) in UCP1 KI pigs, which is consistent with previous reports that UCP1 overexpression in WAT results in decreased fat deposition in mice (1, 56). Moreover, the CLP was increased significantly as a result of decreased fat accumulation. Notably, our UCP1 transgenic pigs were healthy and showed a normal growth rate, normal activity levels, and no obvious behavioral defects. These beneficial effects of ectopic expression of UCP1 on pig production efficiency and pig physiology must be verified in increased pig numbers and commercial pig breeds.

The molecular basis of the improved fat traits appears to result from increased lipolysis in the WAT, as evidenced by the smaller lipid droplets in WAT, the up-regulated expression of lipolysis proteins, and significantly higher levels of FFAs and lower levels of TGs in plasma. These results are consistent with studies showing that the disruption of UCP1 in mice completely impaired lipolysis (57, 58).

In summary, UCP1 transgenic pigs were generated by a site-specific KI strategy and were cold-tolerant as piglets and had improved carcass quality as adults. The development of this pig model is not only valuable for the alleviation of a major economic and welfare issue but also leads to the improvement of economically important pig meat traits.

Materials and Methods

Ethics Statement and Animal Housing. All experiments involving animals were conducted according to the guidelines for the care and use of laboratory animals established by the Beijing Association for Laboratory Animal Science and approved by the Animal Ethics Committee of the Institute of Zoology, Chinese Academy of Sciences. Pigs were raised at the Beijing Farm Animal Research Center. Feed was given twice daily until 2 mo of age, after which the pigs were fed ad libitum. The pigs and feed were weighed at 1-mo intervals to calculate average daily gain and feed efficiency.

Plasmids. Since no classical BAT was identified in pigs, we planned to express UCP1 in adipocytes of pigs by adiponectin promoter, which has been reported to be exclusively expressed in WAT (59). To construct the targeting vector, mouse UCP1 coding sequence, cloned from mouse BAT cDNA, was ligased with adiponectin promoter. The adiponectin-UCP1 3′ UTR fragment was then cloned into the PLB vector using a lethal-based fast cloning kit (Tiangen Biotech). The resulting plasmid was linearized by BspEI (New England Biolabs) digestion. Finally, the bait sequence was inserted into the linearized plasmid to complete the donor vector. The CRISPR/Cas9 construct was obtained as previously described.

Cell Culture and Transfection. Primary pig PEFs were isolated as previously reported (60). Cas9-gRNA plasmids were cotransfected into cultured PEF cells by nucleofection. Forty-eight hours after transfection, cells were harvested using 0.25% trypsin/EDTA (Gibco), and the cell density was calculated using a handheld automated cell counter (Millipore). Single cells were plated in each well of 96-well plates by limiting dilution and cultured for ∼10 d in cell culture medium supplemented with 2.5 ng/mL basic fibroblast growth factor (Sigma). The medium was replaced every 4 d. Confluent cell colonies were propagated and genotyped by PCR and sequencing.

Nuclear Transfer and Embryo Transfer. Pig ovaries were collected from a local slaughterhouse and transported to the laboratory within 1 h in 0.9% saline maintained at 37 °C. The in vitro maturation of oocytes, enucleation, microinjection, and the fusion of reconstructed oocytes were performed in our laboratory according to previously described methods (60). The reconstructed embryos were cultured in porcine zygote medium in 5% CO_2 at 39 °C for 14–16 h until embryo transfer. Embryos in good condition were surgically transferred into the oviduct of a surrogate the day after observed estrus. Gestation was detected by ultrasound at day 28 after embryo transfer. All of the cloned piglets were delivered by natural birth.

PET. Data were acquired for all studies in this work using a whole-body PET scanner (Judicious PET L900), which was developed by the Institute of High Energy Physics, Chinese Academy of Sciences. The scanner uses LYSO-based detector blocks with a 70-cm transaxial field of view (FOV) and a 21.6-cm axial FOV. According to National Electrical Manufacturers Association NU 2-2007 procedures, the transverse (axial) spatial resolution FWHM values were measured as 4.4 (3.9) mm and 5.1 (4.0) mm at 1 cm and 10 cm off-axis, respectively, and the sensitivity average at 0 cm and 10 cm was 13.2 cps/kBq. The emission projection data were acquired in list-mode format and were Fourier-rebinned into 2D sinograms. Images were then reconstructed using the 2D ordered subsets expectation maximization (OSEM) algorithm (four iterations and 16 subsets), which resulted in a $2.0 \times 2.0 \times 1.8\text{-mm}^3$ voxel size for a $320 \times 320 \times 119$-image volume. The PET images were corrected for detector efficiency, dead time, decay, photon scatter, and attenuation.

Cold Challenge Experiment. One-month-old piglets and 6-mo-old pigs were subjected to cold stimulation. One-month-old piglets were placed in a cold chamber (4 °C) for up to 4 h, and 6-mo-old pigs were kept in separate cages in the open air because the air temperature was ∼0 °C at that time. The rectal temperatures of pigs were measured hourly using a rectal probe connected to a digital thermometer (Jinming Instrument Co. Ltd.). Infrared pictures were taken with an infrared camera (FLIR Systems, Inc.). Photographs were processed, and temperatures were quantified using FLIR Tools software.

Porcine Primary Preadipocyte Isolation and in Vitro Differentiation. Adipose tissues were harvested from 2-wk-old piglets, minced, and digested with 2 mg/mL collagenase type I (Sigma) in DMEM/F12 containing 1% fatty acid-free BSA (Sigma) for 60 min at 37 °C. Stromal vascular fraction cells were collected with a cell strainer (70-μm diameter) and then plated and grown in DMEM/F12 (Gibco) supplemented with 10% FBS (Sigma) and 1% penicillin-streptomycin. For white adipocyte differentiation, cells were grown to confluence and then were treated with human WAT induction medium [DMEM/H medium containing 0.25 mM isobutylmethylxanthine, 0.1 μM dexamethasone, 66 nM human insulin (Sigma), 17 μM pantothenate, 33 μM biotin, 20 mM Hepes (pH 7.4), and 0.5% FBS] for 5 d. At day 5, half of the induction medium was removed and the same volume of human WAT mature medium [DMEM/H medium containing 0.1 μM dexamethasone, 66 nM human insulin, 17 μM pantothenate, 33 μM biotin, 20 mM Hepes (pH 7.4), and 10% FBS] was added. One day later, the cells were cultured in pure human WAT maturation medium for 2 d. On day 8, the fully differentiated adipocytes were used for a bioenergetics profiling experiment.

Bioenergetic Profiling. Pig primary s.c. adipocytes were seeded into gelatin-coated XF24 culture microplates (Seahorse Bioscience) and cultured in DMEM/F12 with 10% FBS and antibiotics (100 units/mL penicillin and 100 μg/mL streptomycin) overnight at 37 °C in an atmosphere of 5% CO_2. The next day, the cells were cultured in differentiation medium. On day 8, the O_2 consumption was measured with a Seahorse Bioscience XF24-3 extracellular flux analyzer. To measure OCR independent of oxidative phosphorylation, 1 μM oligomycin was added to cells. Subsequently, 0.5 μM FCCP and 2 μM respiratory chain inhibitor (rotenone) were added to measure the maximal respiration and basal nonmitochondrial respiration rates. Basal oxygen consumption was calculated by baseline oxygen consumption (state 3) minus nonmitochondrial respiration (the minimum of states 10–12). Maximal respiration was calculated by maximal oxygen consumption (the maximum of states 7–9) minus nonmitochondrial respiration (the minimum of states 10–12). The mean and SEM from three independent experiments are shown. Statistical comparisons were made using Student's *t* test.

Physical Activity Measurement. When pigs reached 2 mo old, they were divided into separate pens to measure their physical activity levels. Actigraph GT3x activity monitors on collars were attached to the necks of the pigs to perform the measurement. The activity logger measures the activity in three axes using accelerometers. Axis *x* measures forward/backward acceleration, axis *y* measures sideways acceleration, and axis *z* measures up/down acceleration. The units of measurement are counts integrated across all three

dimensions and reflect the intensity of animal activity (called the vector magnitude). The values were recorded for four KI and four WT pigs at 1-min intervals, and the measurement was performed continuously for 5 d. The data were averaged over each hour and across the groups of KI or WT animals. Data were analyzed using ANOVA with time of day and genotype as factors. Individual was included as a random factor nested within time to account for repeated measurements in the analysis.

DLW. DEE (kilojoules per day) was measured using the DLW technique (25) in a total of 12 pigs (six KI and six WT). This method has been previously validated on multiple occasions by comparison with simultaneous indirect calorimetry in large animals, such as humans, and provides an estimate of energy expenditure with a precision better than 6% (reviewed in ref. 61). On day 1, the animals were weighed (±100 g), and a 100-μL blood sample was obtained to estimate the background isotope enrichments of ^{2}H and ^{18}O (method D in ref. 62). Blood samples were immediately heat-sealed into 2 × 100-μL glass capillaries, which were stored at RT. Afterward, a known mass of DLW (660,000 ppm ^{18}O, 328,000 ppm ^{2}H) was administered intraperitoneally. Syringes were weighed before and after administration (±0.001 g, Sartorius balance) to calculate the exact mass of DLW injected. Blood samples were taken after 1, 2, and 3 h of isotope equilibration to estimate initial isotope enrichments (63). Subsequent samples were collected daily as closely as possible to multiples of 24 h to avoid circadian effects (64). Animals were measured over 5 d. Making measurements across multiple days minimizes the large day-to-day variability in DEE. The analysis of the isotopic enrichment of blood was performed blinded to the animal genotype using a Liquid Isotope Water Analyzer (Los Gatos Research). Initially, the blood was vacuum-distilled, and the resulting distillate was used for analysis. Samples were run alongside five laboratory standards for each isotope and international standards to correct delta values to parts per million. Daily isotope enrichments were $\log_e$-converted, and the elimination constants (k_o and k_d) were calculated by fitting a least-squares regression model to the $\log_e$-converted data. The back-extrapolated intercept was used to calculate the isotope dilution spaces (N_o and N_d). These pigs have a body mass that sits in the region where it is not entirely clear from validation studies whether a two-pool or single-pool model should be used to calculate the CO_2 production and corresponding energy expenditure. Data presented in the paper refer to calculations using a two-pool model, specifically, equation A6 from ref. 65, as recommended by Speakman (66) for animals weighing >5 kg. We also calculated the data using a single-pool model (equation 7.17 from ref. 61) to confirm that the outcomes were not affected by the choice of model, as recommended by Speakman and Hambly (67).

qPCR Analysis. Total RNA was isolated from pig adipose tissue with TRIzol (Invitrogen). First-strand cDNA synthesis was performed using a FastQuant RT Kit (Tiangen Biotech). Quantitative real-time PCR reactions were performed using SYBR Premix Ex Taq (TIi RNaseH Plus; Takara) on an Agilent Mx3005p (Agilent Technologies) with reaction volumes of 20 μL. The primer sequences are listed in Table S3. Relative gene expression was calculated using the comparative cycle threshold ($2^{-\Delta\Delta Ct}$) method. Statistical analysis was performed with GraphPad Prism 6.0.

Western Blotting. Fat tissues were dissected, frozen immediately in liquid nitrogen, and stored at −80 °C until use. Total proteins from tissue or cultured adipocyte were extracted using the Minute Total Protein Extraction Kit (Invent Biotechnologies, Inc.). The proteins were subjected to Western blot analysis with the following antibodies: anti-UCP1 for tissues (GTX632673, 1:1,000; GeneTex, Inc.), anti-UCP1 for adipocytes (ab10983, 1:1,000; Abcam), anti-ATGL (2439, 1:2,000; CST), anti-HSL (4107, 1:2,000; CST), anti-pHSL (4139 for Ser563, 4126 for Ser660, 1:2,000; CST), anti-PPARγ (ab45036, 1:2,000; Abcam), and anti-Tubulin (sc-9104, 1:3,000; Santa Cruz Biotechnology). The blots were developed using HRP-conjugated secondary antibodies and an ECL Plus system. All signals were visualized and analyzed with a Tanon 5200 (Tanon Science & Technology Co. Ltd.).

Microscopy. Adipose tissues were excised and fixed in 4% paraformaldehyde and dehydrated overnight in 70% ethanol. The fixed specimens were processed into paraffin blocks, sectioned, and stained with H&E using a standard protocol. Fat cell size was measured using ImageJ (NIH) software. For TEM, adipose tissue sections were fixed in 2% (vol/vol) glutaraldehyde in 100 mM phosphate buffer (pH 7.2) for 12 h at 4 °C. The samples were then postfixed in 1% osmium tetroxide, dehydrated in ascending gradations of ethanol, and embedded in fresh epoxy resin 618. Ultrathin sections (60–80 nm) were cut and stained with lead citrate before being examined on a Philips CM-120 transmission electron microscope.

Ex Vivo Lipolysis Measurement. For ex vivo lipolysis, s.c. and perirenal fat pads (~0.5 g) isolated from pigs were incubated at 37 °C in 1.0 mL of phenol red-free DMEM containing 2% fatty acid-free BSA with or without 1 μmol/L isoproterenol. The concentrations of glycerol (EAPL-200; BioAssay Systems) in incubation media were quantified according to the manufacturer's protocols.

Blood Lipid Analysis. After collecting blood samples, serum from each pig was prepared and stored at −80 °C until use. Total serum levels of TGs and FFAs were measured in the 306th Hospital of People's Liberation Army of China (Beijing, China).

Carcass Trait Measurements. The pigs were fasted for 24 h before slaughter and anesthetized to death. At slaughter, the carcass was split longitudinally, and the head, hair, feet, and viscera (except for leaf fat and kidney) were removed. The CW was recorded. The dressing percentage for an individual animal was defined as the CW divided by the live weight. Measurements of BFT at the midline were conducted with a Vernier caliper at the scapular margin, the last rib, and the lumbosacral junction, and the average BFT of the three points was used. Measurements of the longissimus muscle area were conducted on the cut surface at the intercostal space between the 10th and 11th ribs by planimeter. Because the BFT was strongly correlated with the body weight, all of the measured BFT data were converted to those of 20-kg body weight according to the regression equation established at our own farm: $BFT = 6.218 + 0.2125BW$ ($R^2 = 0.7884$), where BW is body weight. The left half of the carcass was dissected to lean meat, fat, skin, and bone. The percentage of each part was calculated by dividing each by the weight of the left half of the carcass.

Statistical Analysis. The statistical data reported include results from at least three biological replicates. All results are expressed as the mean ± SEM. For normal distribution data, differences between two groups were assessed by unpaired Student's *t* tests.

ACKNOWLEDGMENTS. We thank members of the J.Z., W.J., and Y.W. laboratories for helpful discussions; P. Chai, S. Liu, H. Tang, and C. Wei (Institute of High Energy Physics at the Chinese Academy of Sciences and Beijing Engineering Research Center of Radiographic Techniques and Equipment) for their help with the PET scan experiments and analysis; L. Yang (Institute of Genetics and Developmental Biology at the Chinese Academy of Sciences) for help in TEM analysis; and Peter Thomson (University of Aberdeen) for technical assistance with isotope analysis. This study was supported by the National Transgenic Project of China (Grant 2016ZX08009003-006-007), the Strategic Priority Research Programs of the Chinese Academy of Sciences (Grants XDA08010304 and XDB13030000), the National Natural Science Foundation of China (Grants 81671274 and 31272440), and the National Program on Key Basic Research Project (973 Program; Grant 2015CB943100). Y.W. was supported by the Elite Youth Program of the Chinese Academy of Agricultural Sciences (ASTIP-IAS05).

1. Kopecky J, Clarke G, Enerbäck S, Spiegelman B, Kozak LP (1995) Expression of the mitochondrial uncoupling protein gene from the aP2 gene promoter prevents genetic obesity. *J Clin Invest* 96:2914–2923.
2. Wang W, Seale P (2016) Control of brown and beige fat development. *Nat Rev Mol Cell Biol* 17:691–702.
3. Li B, et al. (2000) Skeletal muscle respiratory uncoupling prevents diet-induced obesity and insulin resistance in mice. *Nat Med* 6:1115–1120.
4. Lowell BB, et al. (1993) Development of obesity in transgenic mice after genetic ablation of brown adipose tissue. *Nature* 366:740–742.
5. Garruti G, Ricquier D (1992) Analysis of uncoupling protein and its mRNA in adipose tissue deposits of adult humans. *Int J Obes Relat Metab Disord* 16: 383–390.
6. Lowell BB, Flier JS (1997) Brown adipose tissue, beta 3-adrenergic receptors, and obesity. *Annu Rev Med* 48:307–316.
7. Villarroya F, Cereijo R, Villarroya J, Giralt M (2017) Brown adipose tissue as a secretory organ. *Nat Rev Endocrinol* 13:26–35.
8. McGaugh S, Schwartz TS (2017) Here and there, but not everywhere: Repeated loss of uncoupling protein 1 in amniotes. *Biol Lett* 13:20160749.
9. Trayhurn P, Temple NJ, Van Aerde J (1989) Evidence from immunoblotting studies on uncoupling protein that brown adipose tissue is not present in the domestic pig. *Can J Physiol Pharmacol* 67:1480–1485.
10. Berg F, Gustafson U, Andersson L (2006) The uncoupling protein 1 gene (UCP1) is disrupted in the pig lineage: A genetic explanation for poor thermoregulation in piglets. *PLoS Genet* 2:e129.
11. Lin J, et al. ((May 9, 2017) Cold adaptation in pigs depends on UCP3 in beige adipocytes. *J Mol Cell Biol*, 10.1093/jmcb/mjx018.
12. Hou L, et al. (2017) Pig has no uncoupling protein 1. *Biochem Biophys Res Commun* 487:795–800.

13. Kirkden RD, Broom DM, Andersen IL (2013) Invited review: Piglet mortality: Management solutions. *J Anim Sci* 91:3361–3389.
14. Algers B, Jensen P (1990) Thermal microclimate in winter farrowing nests of free-ranging domestic pigs. *Livest Prod Sci* 25:177–181.
15. Jastroch M, Andersson L (2015) When pigs fly, UCP1 makes heat. *Mol Metab* 4: 359–362.
16. Zhou H, Xin H (1998) Responses of piglets to variable and constant wattage heat lamps with clear or red-color radiant rays. *Swine Research Report*. Available at http://lib.dr.iastate.edu/swinereports_1997/18. Accessed August 8, 2017.
17. Wood JD, et al. (2008) Fat deposition, fatty acid composition and meat quality: A review. *Meat Sci* 78:343–358.
18. Patience JF, Rossoni-Serão MC, Gutiérrez NA (2015) A review of feed efficiency in swine: Biology and application. *J Anim Sci Biotechnol* 6:33.
19. Cong L, et al. (2013) Multiplex genome engineering using CRISPR/Cas systems. *Science* 339:819–823.
20. Hai T, Teng F, Guo R, Li W, Zhou Q (2014) One-step generation of knockout pigs by zygote injection of CRISPR/Cas system. *Cell Res* 24:372–375.
21. Li J, et al. (2015) Intron targeting-mediated and endogenous gene integrity-maintaining knockin in zebrafish using the CRISPR/Cas9 system. *Cell Res* 25:634–637.
22. Wang X, et al. (2016) One-step generation of triple gene-targeted pigs using CRISPR/Cas9 system. *Sci Rep* 6:20620.
23. Virtanen KA, et al. (2009) Functional brown adipose tissue in healthy adults. *N Engl J Med* 360:1518–1525.
24. Cypess AM, et al. (2009) Identification and importance of brown adipose tissue in adult humans. *N Engl J Med* 360:1509–1517.
25. Butler PJ, Green JA, Boyd IL, Speakman JR (2004) Measuring metabolic rate in the field: The pros and cons of the doubly labelled water and heart rate methods. *Funct Ecol* 18:168–183.
26. Tschöp MH, et al. (2011) A guide to analysis of mouse energy metabolism. *Nat Methods* 9:57–63.
27. Schulz TJ, Tseng YH (2013) Brown adipose tissue: Development, metabolism and beyond. *Biochem J* 453:167–178.
28. Dempersmier J, et al. (2015) Cold-inducible Zfp516 activates UCP1 transcription to promote browning of white fat and development of brown fat. *Mol Cell* 57:235–246.
29. Barrangou R, Doudna JA (2016) Applications of CRISPR technologies in research and beyond. *Nat Biotechnol* 34:933–941.
30. Whitworth KM, et al. (2016) Gene-edited pigs are protected from porcine reproductive and respiratory syndrome virus. *Nat Biotechnol* 34:20–22.
31. Ruan J, et al. (2015) Highly efficient CRISPR/Cas9-mediated transgene knockin at the H11 locus in pigs. *Sci Rep* 5:14253.
32. Capecchi MR (2005) Gene targeting in mice: Functional analysis of the mammalian genome for the twenty-first century. *Nat Rev Genet* 6:507–512.
33. Peng J, et al. (2015) Production of human albumin in pigs through CRISPR/Cas9-mediated knockin of human cDNA into swine albumin locus in the zygotes. *Sci Rep* 5:16705.
34. Lai S, et al. (2016) Generation of knock-in pigs carrying Oct4-tdTomato reporter through CRISPR/Cas9-mediated genome engineering. *PLoS One* 11:e0146562.
35. Cannon B, Nedergaard J (2004) Brown adipose tissue: Function and physiological significance. *Physiol Rev* 84:277–359.
36. Symonds ME, Lomax MA (1992) Maternal and environmental influences on thermoregulation in the neonate. *Proc Nutr Soc* 51:165–172.
37. Wischner D, Kemper N, Krieter J (2009) Nest-building behaviour in sows and consequences for pig husbandry. *Livest Sci* 124:1–8.
38. Executive BP (2011) *Pig Yearbook 2011* (Agriculture and Horticulture Development Board, Kenilworth, UK).
39. Baxter E, et al. (2013) The welfare implications of large litter size in the domestic pig II: Management factors. *Anim Welfare* 22:219–238.
40. Zhou H, Xin H (1999) Effects of heat lamp output and color on piglets at cool and warm environments. *Appl Eng Agric* 15:327–330.
41. Theil PK, Lauridsen C, Quesnel H (2014) Neonatal piglet survival: Impact of sow nutrition around parturition on fetal glycogen deposition and production and composition of colostrum and transient milk. *Animal* 8:1021–1030.
42. Enerbäck S, et al. (1997) Mice lacking mitochondrial uncoupling protein are cold-sensitive but not obese. *Nature* 387:90–94.
43. Messias de Bragan ca M, Mounier AM, Prunier A (1998) Does feed restriction mimic the effects of increased ambient temperature in lactating sows? *J Anim Sci* 76:2017–2024.
44. Quiniou N, Noblet J (1999) Influence of high ambient temperatures on performance of multiparous lactating sows. *J Anim Sci* 77:2124–2134.
45. Hamann A, Flier JS, Lowell BB (1996) Decreased brown fat markedly enhances susceptibility to diet-induced obesity, diabetes, and hyperlipidemia. *Endocrinology* 137: 21–29.
46. Qiang L, et al. (2012) Brown remodeling of white adipose tissue by SirT1-dependent deacetylation of Pparγ. *Cell* 150:620–632.
47. Takahashi A, et al. (2015) Post-transcriptional stabilization of Ucp1 mRNA protects mice from diet-induced obesity. *Cell Rep* 13:2756–2767.
48. Vijgen GH, et al. (2012) Increase in brown adipose tissue activity after weight loss in morbidly obese subjects. *J Clin Endocrinol Metab* 97:E1229–E1233.
49. Vijgen GH, et al. (2011) Brown adipose tissue in morbidly obese subjects. *PLoS One* 6: e17247.
50. Knecht D, Duziński K (2016) The effect of sex, carcass mass, back fat thickness and lean meat content on pork ham and loin characteristics. *Arch Anim Breed* 59:51–57.
51. Jacyno E, Pietruszka A, Kawęcka M, Biel W, Kotodziej-Skalska A (2015) Phenotypic correlations of backfat thickness with meatiness traits, intramuscular fat, longissimus muscle cholesterol and fatty acid composition in pigs. *S Afr J Anim Sci* 45:122–128.
52. Lopez-Bote CJ (1998) Sustained utilization of the Iberian pig breed. *Meat Sci* 49(Suppl 1):S17–S27.
53. Ai H, et al. (2012) Detection of quantitative trait loci for growth- and fatness-related traits in a large-scale White Duroc × Erhualian intercross pig population. *Anim Genet* 43:383–391.
54. Jiang YZ, et al. (2012) Carcass and meat quality traits of four commercial pig crossbreeds in China. *Genet Mol Res* 11:4447–4455.
55. Lowe BK, et al. (2014) Effects of feeding ractopamine hydrochloride (Paylean) to physical and immunological castrates (Improvest) in a commercial setting on carcass cutting yields and loin quality. *J Anim Sci* 92:3715–3726.
56. Rossmeisl M, et al. (2002) Expression of the uncoupling protein 1 from the aP2 gene promoter stimulates mitochondrial biogenesis in unilocular adipocytes in vivo. *Eur J Biochem* 269:19–28.
57. Dong M, et al. (2013) Cold exposure promotes atherosclerotic plaque growth and instability via UCP1-dependent lipolysis. *Cell Metab* 18:118–129.
58. Mottillo EP, et al. (2014) Coupling of lipolysis and de novo lipogenesis in brown, beige, and white adipose tissues during chronic β3-adrenergic receptor activation. *J Lipid Res* 55:2276–2286.
59. Wang ZV, Deng Y, Wang QA, Sun K, Scherer PE (2010) Identification and characterization of a promoter cassette conferring adipocyte-specific gene expression. *Endocrinology* 151:2933–2939.
60. Yao J, et al. (2014) Efficient bi-allelic gene knockout and site-specific knock-in mediated by TALENs in pigs. *Sci Rep* 4:6926.
61. Speakman JR (1997) *Doubly-Labelled Water: Theory and Practice* (Chapman and Hall, London).
62. Speakman J, Racey P (1987) The equilibrium concentration of oxygen-18 in body water: Implications for the accuracy of the doubly-labelled water technique and a potential new method of measuring RQ in free-living animals. *J Theor Biol* 127:79–95.
63. Król E, Speakman JR (1999) Isotope dilution spaces of mice injected simultaneously with deuterium, tritium and oxygen-18. *J Exp Biol* 202:2839–2849.
64. Speakman J, Racey P (1988) Consequences of non steady-state CO2 production for accuracy of the doubly labelled water technique: The importance of recapture interval. *Comp Biochem Physiol Part A Physiol* 90:337–340.
65. Schoeller DA, et al. (1986) Energy expenditure by doubly labeled water: Validation in humans and proposed calculation. *Am J Physiol* 250:R823–R830.
66. Speakman JR (1993) How should we calculate CO2 production in doubly labeled water studies of animals? *Funct Ecol* 7:746–750.
67. Speakman JR, Hambly C (2016) Using doubly-labelled water to measure free-living energy expenditure: Some old things to remember and some new things to consider. *Comp Biochem Physiol A Mol Integr Physiol* 202:3–9.
68. Zhao J, Zheng Q, Huang J, Qin G, Jin W (2017) Production of transgenic pigs tolerant to cold stimulation with lean phenotype. People's Republic of China Patent Appl 201710323141.0.